Article

Cell Reports

The Long Non-coding RNA HIF1A-AS2 Facilitates the Maintenance of Mesenchymal Glioblastoma Stem-like Cells in Hypoxic Niches

Graphical Abstract

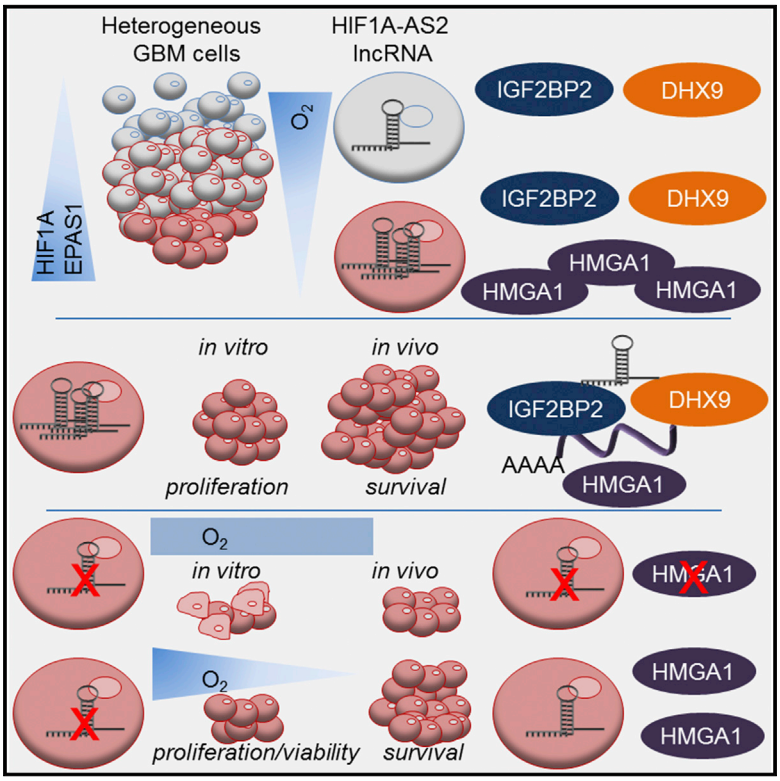

Highlights

- lncRNA signatures reveal tissue and cellular heterogeneity in defined GBM subtypes
- HIF1A-AS2 targets pathways that drive the adaptation to the hypoxic niche in GBM
- HIF1A-AS2 is a mesenchymal GSC-specific lncRNA that promotes tumorigenicity

Authors

Marco Mineo, Franz Ricklefs, Arun K. Rooj, ..., E. Antonio Chiocca, Jakub Godlewski, Agnieszka Bronisz

Correspondence

eachiocca@partners.org (E.A.C.), jgodlewski@partners.org (J.G.), abronisz@partners.org (A.B.)

In Brief

Mineo et al. show that lncRNA HIF1A-AS2 is selectively upregulated in mesenchymal glioblastoma stem-like cells in response to low oxygen. Cellular and molecular rearrangements driven by HIF1A-AS2 and proteins from direct interactome indicate that this lncRNA acts in a tumor anatomic site-dependent fashion to control adaptation to hypoxic stress.

Mineo et al., 2016, Cell Reports *15*, 2500–2509
June 14, 2016
http://dx.doi.org/10.1016/j.celrep.2016.05.018

OPEN ACCESS
CellPress

Cell Reports
Article

The Long Non-coding RNA HIF1A-AS2 Facilitates the Maintenance of Mesenchymal Glioblastoma Stem-like Cells in Hypoxic Niches

Marco Mineo,[1] Franz Ricklefs,[1,2] Arun K. Rooj,[1] Shawn M. Lyons,[3] Pavel Ivanov,[3] Khairul I. Ansari,[1,5] Ichiro Nakano,[4] E. Antonio Chiocca,[1,*] Jakub Godlewski,[1,*] and Agnieszka Bronisz[1,*]

[1]Harvey Cushing Neuro-Oncology Laboratories, Department of Neurosurgery, Brigham and Women's Hospital, Harvard Medical School, Boston, MA 02115, USA

[2]Department of Neurosurgery, University Medical Center Hamburg-Eppendorf, Hamburg 20246, Germany

[3]Division of Rheumatology, Immunology, and Allergy, Brigham and Women's Hospital, Harvard Medical School, Boston, MA 02115, USA

[4]Department of Neurosurgery and Comprehensive Cancer Center, University of Alabama at Birmingham, Birmingham, AL 35243-2823, USA

[5]Present address: Division of Neurosurgery, City of Hope, 1500 East Duarte Road, Duarte, CA 91010, USA

*Correspondence: eachiocca@partners.org (E.A.C.), jgodlewski@partners.org (J.G.), abronisz@partners.org (A.B.)

http://dx.doi.org/10.1016/j.celrep.2016.05.018

SUMMARY

Long non-coding RNAs (lncRNAs) have an undefined role in the pathobiology of glioblastoma multiforme (GBM). These tumors are genetically and phenotypically heterogeneous with transcriptome subtype-specific GBM stem-like cells (GSCs) that adapt to the brain tumor microenvironment, including hypoxic niches. We identified hypoxia-inducible factor 1 alpha-antisense RNA 2 (HIF1A-AS2) as a subtype-specific hypoxia-inducible lncRNA, upregulated in mesenchymal GSCs. Its deregulation affects GSC growth, self-renewal, and hypoxia-dependent molecular reprogramming. Among the HIF1A-AS2 interactome, IGF2BP2 and DHX9 were identified as direct partners. This association was needed for maintenance of expression of their target gene, HMGA1. Downregulation of HIF1A-AS2 led to delayed growth of mesenchymal GSC tumors, survival benefits, and impaired expression of HMGA1 in vivo. Our data demonstrate that HIF1A-AS2 contributes to GSCs' speciation and adaptation to hypoxia within the tumor microenvironment, acting directly through its interactome and targets and indirectly by modulating responses to hypoxic stress depending on the subtype-specific genetic context.

INTRODUCTION

Glioblastoma multiforme (GBM) is the most common and aggressive primary brain tumor in adults, with a median survival of 14.2 months (Johnson and O'Neill, 2012). One of hallmarks of GBM is its high level of heterogeneity with cells exhibiting varying degrees of polymorphism, both phenotypically and molecularly (Soeda et al., 2015). A sub-population of GBM cells has been identified that retains stem cell characteristics, including self-renewal and undifferentiated status, and these cells are described as GBM stem-like cells (GSCs) (Singh et al., 2004). In fact, characterization of the GBM genome (Parsons et al., 2008) and transcriptome (Phillips et al., 2006; Verhaak et al., 2010) has revealed the existence of several distinct cellular subtypes among GBM patients, known as mesenchymal (M), proneural (P), neural (N), and classical (C). Cellular heterogeneity also was demonstrated for pure populations of GSC in culture, based on protein-coding gene expression (Mao et al., 2013), and, recently, single-cell RNA sequencing revealed the co-existence of different GSC subtypes within individual tumors (Patel et al., 2014).

The complexity of solid tumors, including GBM, and their distinct pathophysiology rely on anatomic niches that transmit and receive signals through cellular and acellular mediators (Jones and Wagers, 2008). The GBM microenvironment is a complex ecosystem composed of distinct phenotypic cell components (Patel et al., 2014), including heterogeneous tumor cells (both GSCs and more differentiated progenitor cells), associated astrocytes, infiltrating immune cells and microglia, abnormal vasculature (Meacham and Morrison, 2013), and extensive hypoxic and necrotic zones (Li et al., 2009; Mathew et al., 2014). These components are highly reliant on one another and undergo constant architectural, phenotypic, and transcriptomic re-arrangements, depending on fluctuating microenvironmental contexts as the disease progresses (Godlewski et al., 2015).

In recent years, unprecedented progress has been made toward understanding the function of non-coding RNAs (ncRNAs), which constitute a vast majority of the human transcriptome (Marx, 2014). Among numerous subclasses of ncRNA, a large category is known as long ncRNA (lncRNA). Although poorly described, it is recognized that lncRNAs are capable of tasks such as post-transcriptional regulation, cell-cell signaling, organization of protein complexes, and their allosteric regulation. They are involved in physiological (development and differentiation; Fatica and Bozzoni, 2014) as well as pathological processes, such as carcinogenesis (Huarte, 2015). Several lncRNAs

have been described in hypoxia-associated cancer processes, implying a potential role in maintaining cellular homeostasis and enabling adaptive survival during hypoxia (Chang et al., 2016; Takahashi et al., 2014). lncRNAs are involved in numerous brain functions (Qureshi and Mehler, 2012) and have been increasingly implicated in the pathobiology of GBM (Pastori et al., 2015; Vassallo et al., 2016; Zhang et al., 2013). lncRNAs that are associated with GBM subtypes and clinical prognosis have been identified through integrative analysis of their expression profiles and clinical outcome (Du et al., 2013). Although this analysis predicted lncRNAs that could be potential drivers of cancer progression, it lacked functional validation.

Elucidating the biological mechanisms whereby hypoxic tumor cells can adapt and survive under severe conditions is of significant clinical importance. While it has been widely accepted that proteins and microRNAs take part in hypoxic cancer progression, it is not known if and how lncRNAs participate. Here we report that the lncRNA HIF1A-AS2 is highly expressed in M GSCs and in GBM, but it is largely absent in adjacent brain. HIF1A-AS2 interacts with proteins such as insulin-like growth factor 2 mRNA-binding protein 2 (IGF2BP2) and ATP-dependent RNA helicase A (DHX9), enhancing the expression of several of their targets (e.g., high mobility group AT-hook 1 [HMGA1]), and further downstream leads to changes in endothelial PAS domain-containing protein 1 (EPAS1, also known as HIF2A) expression and the molecular response to hypoxic stress. Remarkably, HIF1A-AS2 regulates the growth and self-renewal of M GSCs, and this phenotype is reflected by gene expression rearrangements that are associated with clinical outcome. Finally, we demonstrate that HIF1A-AS2 is essential for tumorigenicity of M GSC-originated intracranial xenografts and that its expression is stimulated in vivo by hypoxic stress. These results highlight a critical role for HIF1A-AS2 in the maintenance of M GSC function, and they suggest that this lncRNA in GBM mediates the adaptation of GSCs to hypoxic stress.

RESULTS

lncRNA Signature Reflects Intratumoral Heterogeneity of GBM

Recognizing molecular determinants, such as lncRNAs, that act in GSC subtypes would allow identification of functional targets and provide much-needed insight into the contribution of lncRNAs to GBM pathophysiology. To analyze the expression of cancer-related lncRNAs in GBM, we designed a platform (Table S1; Supplemental Experimental Procedures) to detect 73 cancer-related transcripts. We used our collection of GBM specimens to screen lncRNAs, expressed in tumor tissue and in adjacent, matched (i.e., harvested from the same individual) brain tissue. In parallel, we isolated GSCs from GBM specimens and cultured them in serum-free conditions as described before (Peruzzi et al., 2013) (Figure 1A).

The analysis of lncRNA in GBM tissue revealed a tumor-specific pattern of expression: eight lncRNAs were specifically downregulated while seven were specifically upregulated in tumor, when compared to adjacent tissue (Figure 1B, left). The GSC collection was characterized using a gene signature that assigns a GSC culture to P, M, or other subtype (Mao et al., 2013) (Figure S1A). The analysis of lncRNA expression in those GSCs also uncovered a subtype-specific pattern of expression: 20 of 64 detectable lncRNA transcripts (Figure S1B) were significantly enriched in P GSCs and seven were upregulated in M GSCs (Figure 1B, right). The lncRNA HIF1A-AS2 was one of the most differentially expressed in both tissues and cells (Figure 1C, top). In fact there was significant enrichment of HIF1A-AS2 in each GBM compared to its matched brain tissue (Figure 1C, bottom left), as well as in M compared to P GSCs (Figure 1C, bottom right). To validate the platform results, we analyzed the expression of three other lncRNAs that were expressed in GSCs, P-specific MEG3, M-specific WT1-AS, and a non-subtype-specific MALAT1 (Figure S1C). These results show that there were GBM-specific and GBM stem cell subtype-specific patterns of lncRNA expression and that HIF1A-AS2 was one of the most tumor- and subtype-specific lncRNAs.

HIF1A-AS2 Controls Cellular Fate and Molecular Landscape of M GSCs

We hypothesized that HIF1A-AS2 de-regulation may have important implications for the pathobiology of GBM. Lentiviral short hairpin RNA (shRNA)-mediated knockdown of HIF1A-AS2 resulted in its significant depletion in M GSCs (Figure 2A) and significant impairment of growth with a concomitant decrease in cell viability (Figures 2B and S2A). Moreover, HIF1A-AS2 knockdown led to diminished neurosphere-forming capacity and reduced neurosphere size (Figures 2C and 2D). However, targeting of HIF1A-AS2 had little effect on growth or viability of P GSCs (Figure S2B).

To delineate the extent of the HIF1A-AS2-dependent molecular footprint, we used the Nanostring (NS) nCounter PanCancer Pathway Panel that detects transcripts of cancer-related genes. We observed significant de-regulation of 47/730 transcripts (Figures 2E and S2C, top). Interestingly, the majority of upregulated genes were not P or M, while genes downregulated by HIF1A-AS2 knockdown were expressed in P or M GSCs. (Figure S2C, bottom). The in silico analysis revealed marked downregulation of pro-proliferative traits concomitant with upregulation of cell death-related processes in HIF1A-AS2 knockdown M GSCs (Figure S2D). This prompted us to test whether genes de-regulated by HIF1A-AS2 were associated with GBM patient outcome. Despite using a pre-selected (biased) list of genes, we were able to detect significant association of genes downregulated in knockdown cells with poorer outcome (Figure S2E).

The physical proximity of the HIF1A-AS2 to the hypoxia-inducible factor 1 alpha (HIF1A) genomic locus prompted us to test the effect of low oxygen tension on HIF1A-AS2 transcription. This revealed that, in M GSCs, HIF1A-AS2 was not only the most significantly upregulated lncRNA despite its high basal (normoxic) levels but also one of the very few lncRNAs whose levels were affected by hypoxic stress in GSCs (Figure 2F, middle; Table S2), while in P GSCs the levels of HIF1A-AS2 remained low regardless of oxygen concentration. This result was confirmed by qPCR analysis, showing consistent upregulation across all tested M GSCs but not P GSCs (Figure 2F, bottom). Expectedly, levels of HIF1A and EPAS1 mRNA remained stable upon exposure to hypoxic stress in M GSCs (with no apparent pattern in P GSCs), whereas the respective encoded proteins

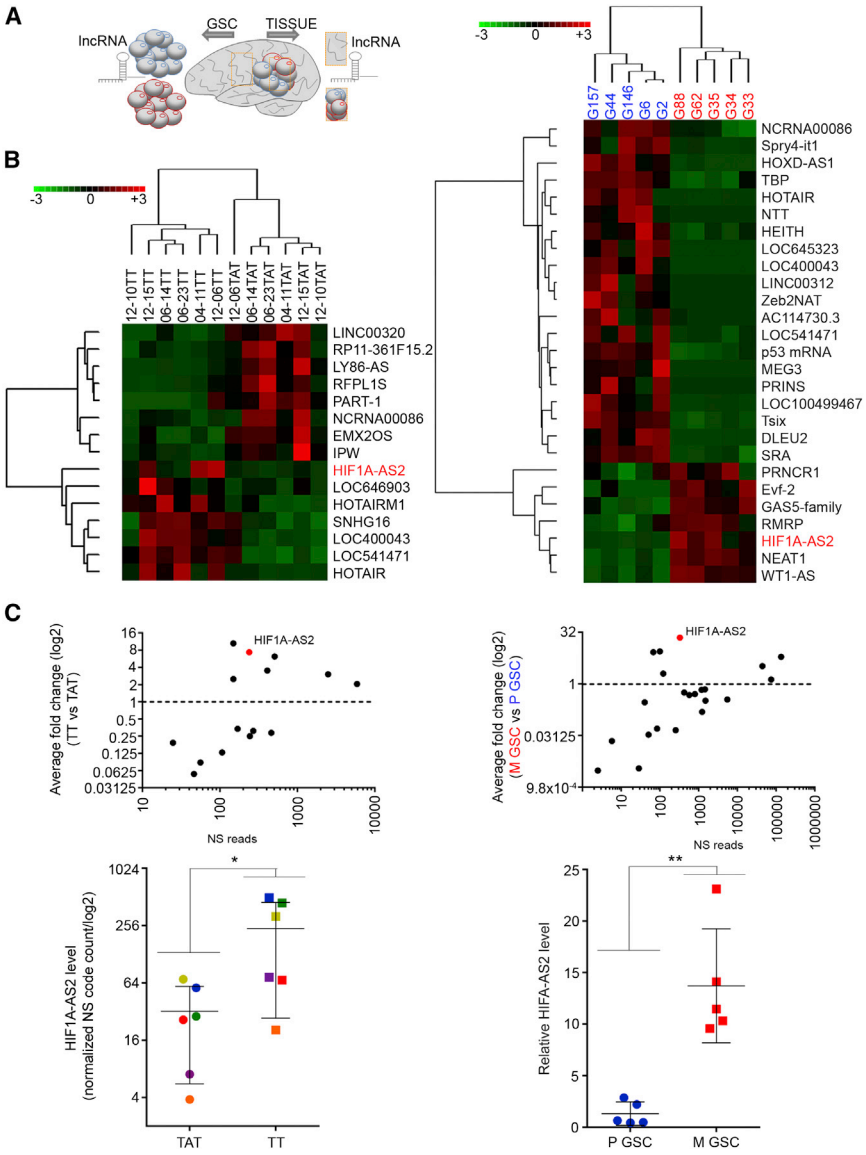

Figure 1. lncRNA Signature Reflects Intratumoral Heterogeneity of GBM

(A) Workflow depicts the isolation of tissue and GSCs from GBM patients for lncRNA analysis.

(B) GBM and GSC lncRNA profile distinguishes tumor tissue (TT) from normal tissue (matched tissue adjacent to brain tumor, TAT) and proneural (P, blue) from mesenchymal (M, red) GSC subtypes. lncRNA sets that vary coherently between tissues (left) and GSCs (right) were identified by supervised clustering (fold > 2, $p < 0.05$).

(C) HIF1A-AS2 is tumor- (left) and M GSC- (right) enriched lncRNA. Relative expression of all lncRNAs (top) and HIF1A-AS2 (bottom) is shown as Nanostring (NS reads) or qPCR. Data are shown as mean ± SD (*$p < 0.05$, **$p < 0.01$).

were consistently induced in both subtypes of GSCs (Figure S2F). Thus, the observed unaltered proliferation and viability in both P and M GSCs under hypoxic stress (Figure S2G) underline the M GSC-specific HIF1A-AS2-driven program.

This effect was not limited to the stem-like cells, as differentiation-promoting conditions did not abolish HIF1A-AS2 expression or its upregulation in hypoxia (Figure S2H) and also led to maintenance of the phenotypic effect of HIF1A-AS2 knockdown (Figure S2I).To assess HIF1A-AS2-dependent signaling during hypoxia, we measured the dynamics of activation of several genes that were shown to be hypoxia dependent in GBM (Patel et al., 2014). The activation of these genes either lagged or did not occur in M GSCs, where HIF1A-AS2 was knocked down (Figure 2G). Moreover, knockdown of HIF1A-AS2 did not alter the induction of HIF1A upon exposure to hypoxia, while induction of EPAS1 was significantly impaired upon HIF1A-AS2 knockdown (Figure 2H). The hypoxic stress caused swift and robust upregulation of HIF1A-AS2 in M GSCs, and a similar but weaker effect was observed in knockdown cells, suggesting that hypoxia-dependent induction of the endogenous transcript overcame the shRNA effects (Figure S2J). Similar to previous findings, HIF1A-AS2 in M GSCs was predominantly nuclear and this distribution was not affected by hypoxic stress (Figure S2K). Knockdown of HIF1A-AS2 resulted in an altered M GSCs phenotype concomitant with hypoxia-dependent molecular rearrangements and de-regulation of genes associated with worse patient outcome, underlining the clinical relevance of this lncRNA in GBM.

HIF1A-AS2 Drives Tumor Progression in a Hypoxic Environment

GBM patients with the aggressive and predominantly M subtype exhibit a particularly high degree of tumor necrosis (Verhaak et al., 2010), and, conversely, highly necrotic tumors are significantly enriched for the M transcriptional gene signature (Cooper et al., 2012). To validate the impact of HIF1A-AS2 on tumorigenicity of GSCs, we implanted highly aggressive M GSCs that expressed either control shRNA or HIF1A-AS2 shRNA as intracranial xenografts (Figure 3A). We sacrificed one group of mice after 10 days while the second group was observed for survival analysis. We observed strikingly smaller tumors in the knockdown group after 10 days (Figures 3B and S3A). The survival benefits in the knockdown group were also significant, although ultimately these mice perished (Figure 3C). We hypothesized that, as tumor growth progresses and hypoxia increases in the tumor core, the effect of shRNA was overridden by increased HIF1A-AS2 expression driven by the hypoxic microenvironment in vivo. This resulted in ultimate tumor progression and only modest survival benefits. Thus, we analyzed the expression of

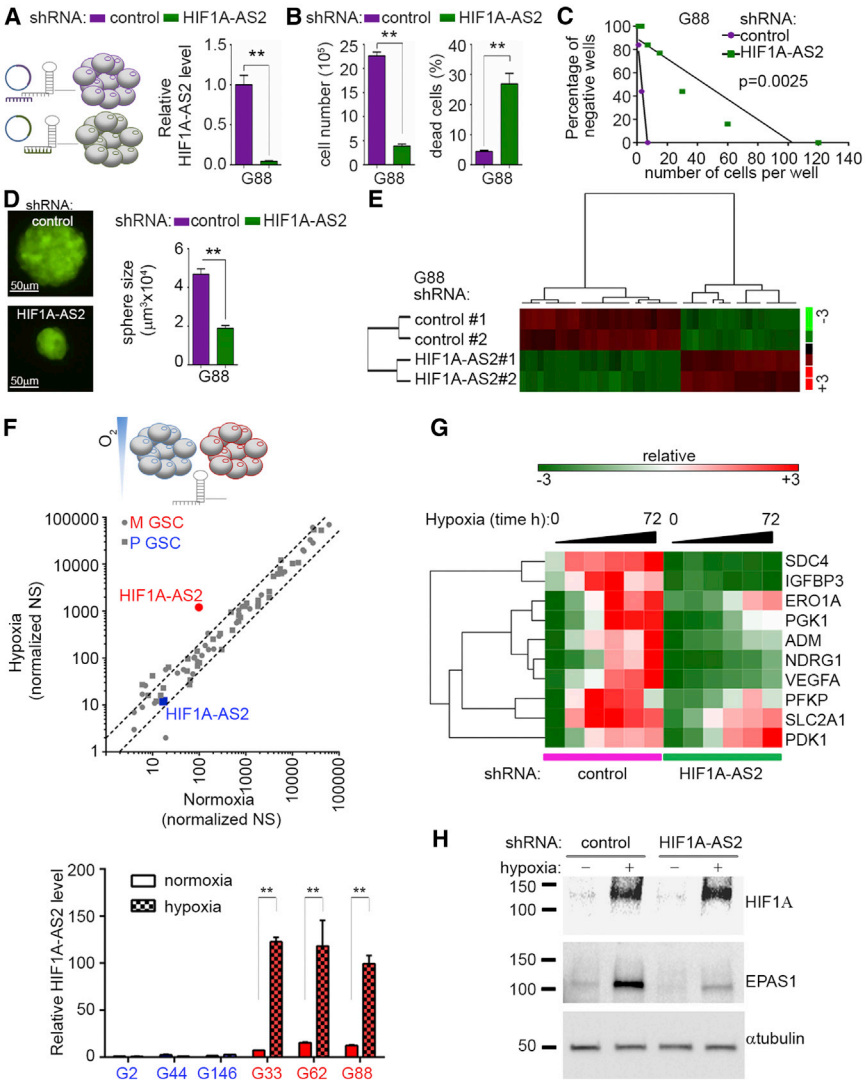

Figure 2. HIF1A-AS2 Controls Cellular Fate and Molecular Landscape of M GSCs

(A) Downregulation of HIF1A-AS2 in M GSCs. Short hairpin (sh)RNA strategy (left) and qPCR analysis are shown (right). Data are shown as mean ± SD (**$p < 0.01$).

(B) Knockdown of HIF1A-AS2 reduces M GSC proliferation (left) and viability (right). Cell number and percentage of dead cells are shown. Data are shown as mean ± SD (**$p < 0.01$).

(C) Knockdown of HIF1A-AS2 inhibits sphere formation. Sphere frequency using linear regression plot is shown.

(D) Knockdown of HIF1A-AS2 reduces sphere growth. Representative microphotographs of GSC spheroids (left) and quantification of sphere volume (right) are shown. Data are shown as mean ± SD (**$p < 0.01$). Scale bar represents50 μm.

(E) Knockdown of HIF1A-AS2 results in gene expression rearrangement. Gene sets that vary coherently between control and HIF1A-AS2 knockdown M GSCs (two single-cell clones 1 and 2 were analyzed) were identified by supervised clustering (fold > 2, $p < 0.05$).

(F) Hypoxic stress upregulates HIF1A-AS2 in M GSCs. Workflow depicts the hypoxic stress strategy (top). Global expression of lncRNAs in normoxic versus hypoxic conditions (middle) is shown (dashed lines indicates 2-fold deregulation). The qPCR validation of HIF1A-AS2 levels in M and P GSCs upon exposure to hypoxia (bottom) is shown. Data are shown as mean ± SD (**$p < 0.01$).

(G) Knockdown of HIF1A-AS2 alters the response to hypoxia. The qPCR-based expression signature is shown.

(H) Knockdown of HIF1A-AS2 suppresses EPAS1 activation. Representative western blot analysis is shown.

HIF1A-AS2, HIF1A, and EPAS1 in vivo. As expected, the expression of both HIF1A and EPAS1 was much weaker in the HIF1A-AS2 knockdown versus control tumors (Figure 3D, left). However, de-repression of the expression of HIF1A-AS2 in knockdown cells occurred in a time-dependent fashion (in agreement with a similar finding in vitro; Figure S2G), and in terminal tumors it reached levels that were comparable to those in control cells (Figure 3D, right). These findings implied that HIF1A-AS2 knockdown tumors delayed their initiation phase (resulting in overall survival benefits), albeit only transiently due to an ultimate increase of hypoxic stress that de-repressed HIF1A-AS2 expression.

HIF1A-AS2 Interactome Targets Belong Predominantly to a Class of RNA-Processing Proteins

To identify the HIF1A-AS2 interactome in M GSCs, we utilized an in vitro transcription assay coupled with transcript biotinylation to allow pull-down of putative targets, followed by mass spectrometry (MS) with additional controls of either no RNA probe or other lncRNA (Figure 4A). We identified a number of putative interacting partners (Table S3), with post-transcriptional regulation of gene expression and mRNA stabilization being the most predominant biological processes (Figure S4A). To validate MS results, we performed western blot analysis on RNA pull-down material (Figure 4B, left). Identification of direct binding partners of HIF1A-AS2 was achieved by UV-mediated cross-linking, followed by RNA pull-down in high-stringency conditions (Figure 4B, right). We identified two proteins, DHX9 and IGF2BP2, that directly interact with HIF1A-AS2 (Figure 4B, right), but not with another lncRNA, MEG3 (Figure 4B, bottom). The specificity of the HIF1A-AS2-DHX9/IGF2BP2 interactions was additionally validated by protein-RNA immunoprecipitation assays using a panel of lncRNAs (P specific: DLEU2 and MEG3; M specific: WT1AS, NEAT1, PRNCR1, GAS5, and RMRP; and GBM specific: MALAT1). This showed that only HIF1A-AS2 physically interacted with these two proteins and that DLEU2, MALAT1, and WT1AS were found to interact only with IGF2BP2, although with lower affinity (Figure S4B). Interestingly, DHX9 and IGF2BP2 have been shown to interact with each other (Chatel-Chaix et al., 2013).

To select potential downstream effectors of HIF1A-AS2, we first determined whether IGF2BP2 targets (Janiszewska et al.,

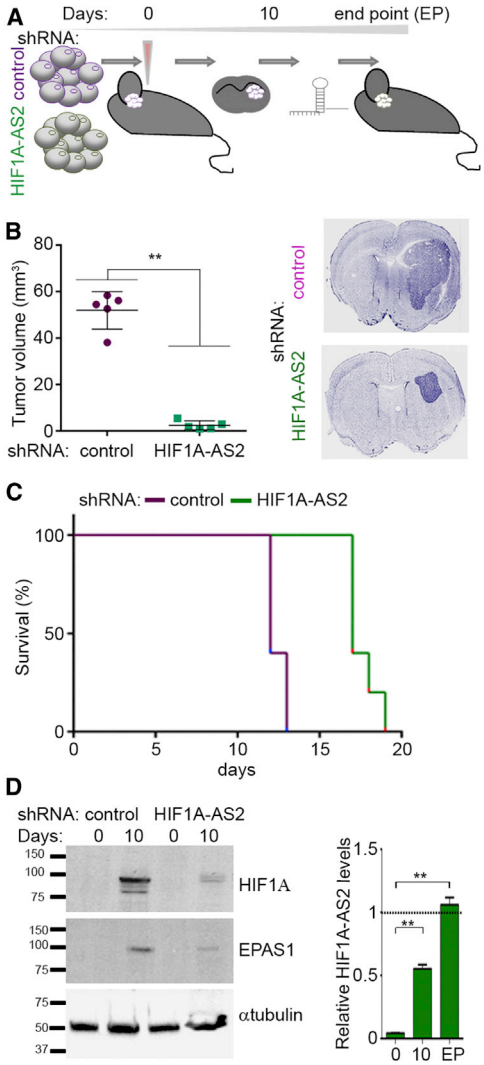

Figure 3. HIF1A-AS2 Drives Tumor Progression in a Hypoxic Environment

(A) Workflow depicts the in vivo experimental design.

(B) HIF1A-AS2 knockdown reduces tumor volume of M GSC-originated intracranial xenografts. Quantification of tumor volume and representative DAPI staining of brain sections 10 days post-implantation are shown. Data are shown as mean ± SD (**$p < 0.01$).

(C) HIF1A-AS2 knockdown in M GSC-originated tumors is associated with prolonged survival. Kaplan-Meier curves are shown (n = 5; p = 0.0023).

(D) Tumor microenvironment effect on HIF1A and EPAS1 expression depends on HIF1A-AS2 status. Representative western blot (left) and qPCR (right) analyses are shown. Expression is relative to control M GSCs. Data are shown as mean ± SD (**$p < 0.01$).

2012) were subtype specific. Given that IGF2BP2 is a protein abundantly expressed in both GSC subtypes, it was not surprising that its target genes were not P or M. Interestingly P GSC-upregulated targets of IGF2BP2 were not subtype specific, in contrast to M GSC genes that overlapped with M signature transcripts (Figure S4C). Among IGF2BP2 target genes, 49 correlated with M GSC-specific expression (Figure S4D, left). Moreover, among IGF2BP2 target genes, there were two genes (HMGA1 and FOS-like antigen 1 [FOSL1]) that were downregulated in both DHX9 knockdown (Figure S4D, right) (Lee et al., 2014) and HIF1A-AS2 knockdown cells (Figure S4D). All nine genes that were targets of IGF2BP2 and HIF1A-AS2 were more abundant in M GSCs (Figure S4E, left). Their downregulation by HIF1A-AS2 knockdown was validated by qPCR (Figure S4E, right).

Next we tested whether binding of HIF1A-AS2 to its protein partners led to functional consequences for their downstream RNA targets (Figure 4C). As expected, there was an interaction between HIF1A-AS2 and DHX9/IGF2BP2 in M GSCs, but not in P GSCs (Figure 4C, left). In addition, we found that in M GSCs there was strong binding between IGF2BP2 and HMGA1, as expected (Janiszewska et al., 2012), and between DHX9 and HMGA1, which has not been previously shown (Figure 4C, middle). Conversely, knockdown of HIF1A-AS2 resulted in significantly diminished interactions between RNA-binding proteins and their mRNA targets (Figure 4C, right). Importantly, knockdown of HIF1A-AS2 did not alter levels of either mRNA or protein of its interacting partners, whereas it significantly suppressed expression of HMGA1 (Figures 4D and S4F). Although the protein levels of DHX9 and IGF2BP2 did not show a significant difference between P and M GSCs, HMGA1 was strongly enriched in M GSCs (Figure S4G).

Finally, we analyzed the expression of HMGA1 in tumors formed by HIF1A-AS2 knockdown cells, and we found that its mRNA and protein levels were significantly elevated in the course of tumor progression (Figure 4E), corresponding with upregulation of HIF1A-AS2 (Figure 3D). Therefore, we conclude that direct interaction of HIF1A-AS2 with DHX9 and IGF2BP2 mRNA-binding complexes drives expression of their downstream mRNA targets with pro-oncogenic functions, such as HMGA1, thus explaining the lncRNA-driven tumorigenic phenotype. As only a certain sub-population of tumor cells expresses HIF1A-AS2 and activates it during hypoxia, we attempted to link the transcriptome profiles of GSC subtypes, HIF1A-AS2 knockdown, and hypoxia to the intratumoral architecture defined by predominant characteristic phenotypes of tumors (infiltration, proliferation, and necrotic zones). As expected, the hypoxic signature was found primarily in necrotic areas, which significantly overlapped with the M signature, but not with the P signature, which was detected mainly in infiltration and proliferation zones. Interestingly, genes downregulated in HIF1A-AS2 knockdown cells were detected predominantly in the necrotic zone (Figure 4F; Table S4). These data implicate HIF1A-AS2 as an lncRNA contributing to GSCs' speciation and adaptation to dynamic oxygen fluctuations in the tumor microenvironment.

DISCUSSION

GSCs are highly tumorigenic and resistant to conventional radio- and chemotherapy; therefore, they constitute the primary target for the development of anti-GBM therapies (Lathia et al., 2015; Sørensen et al., 2015). To date, analyses of molecular diversity have focused mostly on protein-coding genes (Patel et al., 2014), but the engagement and contribution of ncRNAs remain insufficiently characterized.

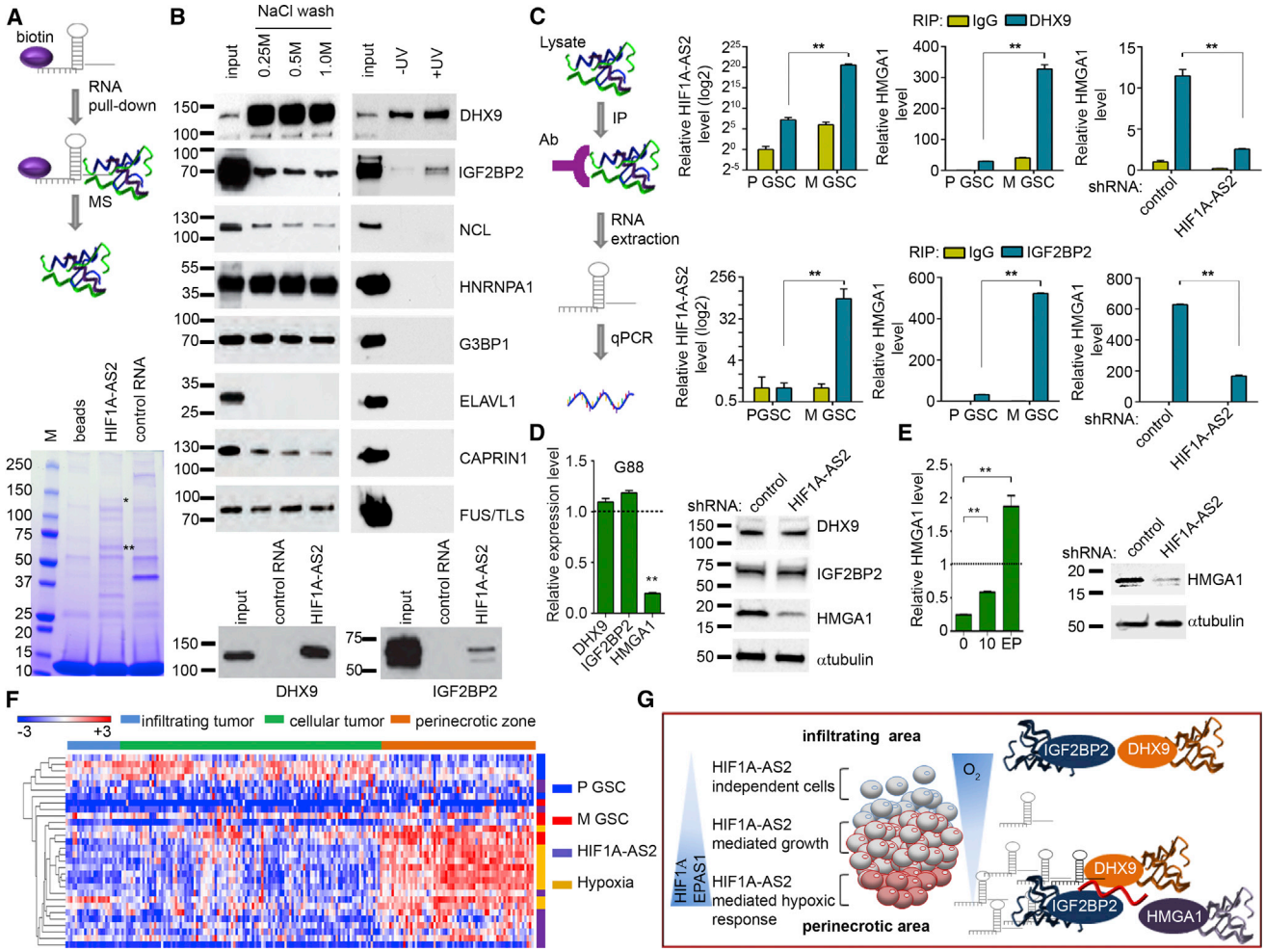

Figure 4. HIF1A-AS2 Interactome Partners Belong to the Class of RNA-Processing Proteins

(A) Workflow depicting approach to identify HIF1A-AS2 interactome in M GSCs by pull-down of biotinylated transcript followed by mass spectroscopy (MS) (top). Coomassie Blue staining of biotinylated HIF1A-AS2-associated proteins is shown (bottom, *DHX9 and **IGF2BP2 band). Binding to other RNA (MEG3) serves as a control of binding specificity.

(B) DHX9 and IGF2BP2 are direct binding partners of HIF1A-AS2. Western blot analysis of a set of proteins identified by MS (left) and UV-crosslinked pull-down of biotinylated HIF1A-AS2 and control RNA (MEG3) are shown (right and bottom).

(C) Binding between HIF1A-AS2 and its interacting partners affects expression of their downstream target HMGA1. Workflow depicts the RNA immunoprecipitation (RIP) strategy (left). Analysis of UV-crosslinked α-DHX9 RIP (top) and α-IGF2BP2 RIP (bottom) and the qPCR in P and M GSCs on HIF1A-AS2 (left) and on HMGA1 (middle) and in control and HIF1A-AS2 knockdown M GSCs (right) are shown. Data are shown as mean ± SD (**$p < 0.01$).

(D) Knockdown of HIF1A-AS2 in M GSCs reduces levels of HMGA1 protein. The qPCR (left) and western blotting analysis (right) of selected genes in M GSCs upon HIF1A-AS2 knockdown are shown. Expression is relative to control M GSCs. Data are shown as mean ± SD (**$p < 0.01$).

(E) HIF1A-AS2 knockdown-dependent suppression of HMGA1 in M GSCs is maintained at the early stage of tumor progression in vivo. The qPCR (left) and western blot (right) analyses of HMGA1 10 days post-implantation in HIF1A-AS2 knockdown M GSCs in vivo are shown. Expression is relative to control M GSCs. Data are shown as mean ± SD (**$p < 0.01$).

(F) Expression of M- or P-specific, hypoxia-dependent and HIF1A-AS2-dependent genes is prevalent in the necrotic niche of GBM. Ivy GAP database-based expression signature in different areas of GBM for top 30 genes is shown.

(G) A proposed HIF1A-AS2-dependent signaling in a normoxic and hypoxic microenvironment of GBM is shown.

Although thousands of lncRNAs have been discovered to date, very little is known about their mode of action and possible role in the regulation of cancer-related processes. The positive correlation of bidirectional sense/antisense transcription is in accord with numerous studies showing that antisense RNAs can regulate their neighboring genes in a *cis* mode (Kunej et al., 2014). Here we have shown that, although HIF1A-AS2 expression responds to hypoxic stress, it had no effect on the expression of its neighboring gene in sense orientation (HIF1A). In fact, the HIF1A locus is ubiquitously transcribed and its protein levels are regulated by rapid degradation under normoxic conditions (Semenza, 2013; Wang et al., 1995). This highly conserved

mechanism is unlikely to be controlled by a cell-type-specific (Thrash-Bingham and Tartof, 1999) and not-conserved (even in mammals) antisense transcript.

One of the prominent modes of action for lncRNAs is to interact with other cellular factors, including proteins, DNA, and other RNA molecules (Minajigi et al., 2015; Ulitsky and Bartel, 2013). The HIF1A-AS2 protein interactome at first indicated a multifunctional role for this lncRNA. We found that identified direct and indirect protein targets were engaged in mRNA metabolism. Interestingly, we did not find that the HIF1A-AS2 lncRNA interacts with transcriptional machinery and protein chromatin-remodeling complexes in GSCs, unlike what has been reported for other lncRNAs (Flynn and Chang, 2012). It remains to be investigated whether a direct interaction of HIF1A-AS2 with DNA or pairing with other RNA molecules can occur. IGF2BP2, the direct binding partner of HIF1A-AS2, has been shown to drive a cancer stem cell phenotype in GBM by binding and stabilizing mRNA (including HMGA1) that is enhanced by hypoxic conditions (Janiszewska et al., 2012), suggesting a possible mechanism for GSC adaptation to low-oxygen environments. In fact, IGF2BP2 mRNA and protein are not deregulated in the various GBM subtypes or by hypoxia, suggesting that its function is regulated by co-interaction with other proteins, such as DHX9. Such interaction already has been shown to be dependent on the presence of RNA (Chatel-Chaix et al., 2013).

Our results suggest that HIF1A-AS2 acts by interacting with RNA-binding proteins (IGF2BP2 and DHX9) to stimulate expression of their target mRNAs, such as HMGA1, resulting in an increase in protein levels. Importantly, in addition to HMGA1's function during development (Chiappetta et al., 1996), it is overexpressed in virtually every cancer (Fusco and Fedele, 2007), and its expression levels correlate with the degree of malignancy. In fact, GBM patients with higher levels of HMGA1 exhibit a significantly shorter progression-free survival time (Liu et al., 2015). Our findings that HIF1A-AS2 (1) is significantly overexpressed in GBM tumors and in M GSCs, (2) promotes stem cell-like and tumorigenic behaviors, and that (3) its expression is associated with GBM outcome suggest that HIF1AS-AS2 is a non-protein-coding oncogene. However, it needs to be noted that HIF1AS-AS2 target genes are highly or even exclusively expressed in M GSC, indicating that HIF1A-AS2 tumorigenic function may be cell specific. It suggests that HIF1A-AS2 may be a contextual oncogene engaged in physiological processes (such as maintenance of homeostasis) in other tissues/organs.

Naturally occurring oxygen gradients serve as morphogenic signals in rapidly growing embryonic tissues (Simon and Keith, 2008), but they become extreme in pathophysiological conditions, such as ischemia or the rise of solid tumors. Thus, chronic exposure to severe oxygen deprivation frequently produces necrotic zones surrounded by densely packed hypoxic tumor cells. This stimulates the development of a tumoral architecture with hierarchical cellular organization/speciation. In fact, our recent study has shown that such cellular organization may be recapitulated in vitro and in vivo (Ricklefs et al., 2016). Interestingly, the gene analysis of GBM tissues harvested by laser microdissection showed a GSC-specific signature associated with tumor anatomic sites (http://glioblastoma.alleninstitute.org) (Figure 4F). Several prominent reports (Bhat et al., 2013; Bozdag et al., 2014; Halliday et al., 2014; Joseph et al., 2015; Nakano, 2014; Piao et al., 2013) have suggested that certain microenvironmental (such as hypoxia) and therapy-inflicted stressors (such as bevacizumab and irradiation) and/or pathway instabilities (VEGF, NF-κB, and TNF) may have caused a transition between GBM subtypes. All these reports, however, provided strong indication of P-to-M transition, while the evidence for the transition occurring in the opposite direction is still lacking. The subtype-specific expression of HIF1A-AS2 that is induced exclusively in M GSCs suggests that this lncRNA drives adaptation of M GSCs to their anatomic hypoxic niche rather than promotes transition shift from one subtype to the other.

The fact that although P GSC do not express HIF1A-AS2 but respond to hypoxia and survive this stress suggests that diverse programs of hypoxic response exist in these cells. The analysis of genes deregulated by HIF1A-AS2 knockdown in M GSCs has shown extensive deregulation; however, a shift toward other subtypes was not observed. In fact, the M-specific signature was downregulated while genes upregulated by HIF1A-AS2 knockdown did not cluster with either subtype. These data, along with the fact that HIF1A-AS2 is not expressed in P GSCs even upon hypoxic stress, indicate that this lncRNA does not take part in a subtype switch, suggesting that P GSCs use a different mechanism for such transition. Characterizing the epigenetic states of phenotypically distinct cells and identifying transcription factors that are sufficient to reprogram differentiated cells into a tumorigenic stem-like state suggest a plastic developmental hierarchy in GBM cell populations (Carro et al., 2010; Suvà et al., 2014).

The recent observation that individual tumors contain a spectrum of GBM subtypes and hybrid cellular states (Patel et al., 2014), which is reflected in the diverse expression of ncRNAs (Du et al., 2013) and range of environmental influences (Godlewski et al., 2015), adds further complexity to the pathobiology of GBM. To fully reconstruct a network model that highlights the critical machinery sufficient to fully reprogram differentiated GBM cells, a comprehensive analysis of transcription factors and their downstream effectors (both protein-coding RNAs and ncRNAs) in the context of the tumor microenvironment is needed. This study shows significant deregulation of lncRNA expression in GBM using highly clinically relevant samples. The clinical significance of our findings was underlined by linking HIF1A-AS2 downstream effectors with patient survival outcomes based on GBM subtypes. It is increasingly evident that GBM/GSC subtypes use different signaling and transcriptional networks (e.g., P GSC-specific Sox2, Olig2, Notch, and PDGFRA and M GSC-specific WT1, c-Met, and EGFR) (Frattini et al., 2013; Mao et al., 2013; Patel et al., 2014). Moreover, GSC subtypes are characterized by divergent epigenetic footprints, as, for example, the activity of Polycomb Repressor Complexes (one of the most important lncRNA effectors) differs significantly between the subtypes (Zheng et al., 2011). Our results clearly indicate that HIF1A-AS2 is selectively important in M GSCs, as its downstream effectors (e.g., HMGA1 and FOSL1) are expressed exclusively in M, but not P, GSCs, providing plausible explanation for its subtype specificity. Importantly, HIF1A-AS2's selective response to hypoxia in M GSCs only, as these cells are found predominantly in hypoxic zones,

suggests that microenvironmental adaptation may be one of important drivers of GSC speciation.

The association between necrosis and the M transcriptional class in GBM highlights the important contribution of the tumor microenvironment in implementation of hierarchical organization of the tumor (Carro et al., 2010; Orr and Eberhart, 2012). Upregulation of HIF1A-AS2 by hypoxia in M, but not P, GSCs suggests that HIF1A-AS2 acting in GBM in a tumor anatomic site-dependent fashion may control adaptation of a specific set of cells to hypoxic stress. Some experimental evidence suggests that tumor cells may cope with hypoxia by turning on the migratory phenotype to escape from metabolically stressful events/locations (Brat et al., 2004). Here we argue that adaptation rather than behavioral transition drives the survival and proliferation of GBM cells in hypoxic zones (Figure 4G).

GBM is recognized as a complex ecosystem composed of cells with distinct phenotypes, genotypes, and epigenetic landscapes. It becomes increasingly clear that the resistance to adverse environmental conditions, such as hypoxia, contributes to the tumor progression and reduced efficacy of anticancer therapies. The mechanisms by which tumor cells respond and adapt to hypoxic stress are crucial in the pathobiology of solid tumors such as GBM. Based on our data, we propose a model depicting an important role for HIF1A-AS2 in the regulation of hypoxic adaptation in tumor cells in a tumor anatomic site-dependent context, which can have important clinical implications and serve as a proof of concept for the development of personalized GBM therapy (Reardon et al., 2015).

EXPERIMENTAL PROCEDURES

Human Specimens

Tumor and tumor-adjacent tissue samples were obtained as approved by the Institutional Review Board at The Ohio State University and Harvard Medical School (HMS). Surgery was conducted by E.A.C. or I.N. Patient samples were processed for extraction of total RNA or establishment of patient-derived neurospheres.

Cell Culture

Primary human GSCs (G2, G6, G33, G34, G35, G44, G62, G88, G146, G157, and G91) were isolated by dissociation of gross tumor samples. The unique identity of cultured patient-derived cells was confirmed by short tandem repeats analysis (Kim et al., 2016). Cells were cultured as neurospheres in stem cell-enriched condition using Neurobasal (Gibco) supplemented with 1% Glutamine (Gibco), 2% B27 (Gibco), and 20 ng/ml epidermal growth factor (EGF) and fibroblast growth factor (FGF)-2 (PeproTech) or in differentiation-promoting condition using DMEM (Gibco) supplemented with 10% fetal bovine serum (FBS, Sigma-Aldrich). For the differentiation effect, cells cultured in stem cell-enriching conditions were transferred to differentiation-promoting conditions. Unless otherwise specified, hypoxia experiments were performed at 1% O_2 for 24 hr. G88, G33, G816, and G44 cell lines were infected with lentiviral psi-LVRU6GP shCTR001 vector or psi-LVRU6GP sh217J6/J8 vectors (GeneCopoeia).

NS Assay

NS nCounter custom-made lncRNA assay and nCounter PanCancer Pathways assay were performed according to the manufacturer's instructions (NanoString Technologies) and as previously described (Peruzzi et al., 2013).

Immunoblot Analysis and Antibodies

Immunoblotting was performed as previously described (Mineo et al., 2012). The following antibodies were used: anti-HIF-1A (610958, BD Biosciences); anti-EPAS1 and anti-HMGA1 (7096 and 7777, respectively, Cell Signaling Technology); anti-DHX9 and anti-IGF2BP2 (A300-855A and A303-316A, respectively, Bethyl Laboratories); anti-NCL, anti-hnRNPA1, anti-G3BP1, anti-HuR (ELAVL1), and anti-Fus/TLS (sc9893, sc10030, sc365338, sc5261, and sc25540, respectively, Santa Cruz Biotechnology); and anti-Caprin1 (15112-1AP, Protein Tech Group).

RNA Pull-Down Assay

Full-length HIF1A-AS2 was cloned into pCI-neo vector (Promega). Biotin-labeled HIF1A-AS2 was transcribed in vitro with Biotin RNA-labeling mix (Roche) and T7 polymerase (Roche) and purified using PureLink RNA Mini kit (Ambion). RNA was heated at 65°C for 5 min and then cooled slowly for 20 min to allow secondary structure formation. GSCs were lysed in lysis buffer (50 mM Tris, 100 mM NaCl, 1% Triton, 1 mM EDTA, 1 mM EGTA, 50 mM beta-glycerophosphate, 1 mM DTT, 1 mM PMSF, and protease inhibitor cocktail). For pull-down assay, 3 μg biotin-labeled HIF1A-AS2 RNA was mixed with total cell lysate (500 μg protein) and incubated at room temperature (RT) for 2 hr in the presence of RNasin (100 U/ml, Promega). Washed streptavidin beads (40 μl, Invitrogen) were added to the binding reaction and further incubated for 1 hr at RT. Beads were washed five times in lysis buffer and bound proteins were analyzed by MS as previously described (Bronisz et al., 2014). For UV-crosslink RNA pull-down assays, the binding reaction was UV irradiated at 400 mJ/cm^2 and then incubated with streptavidin beads at RT. After incubation, beads were washed three times with high-stringency wash buffer, three times in high-salt wash buffer, three times in low-salt wash buffer, three times in PXL buffer (Moore et al., 2014), and three times in lysis buffer. RNA was then digested using RNaseA and bound proteins were analyzed by immunoblotting.

UV-Crosslink RNA Immunoprecipitation

GSCs were UV irradiated at 400 mJ/cm^2 and lysed in modified radio-immunoprecipitation assay (RIPA) buffer (50 mM Tris, 150 mM NaCl, 4 mM EDTA, 1% NP-40, 0.1% Na-deoxycholate, 0.5 mM DTT, 100 U/ml RNasin, protease, and phosphatase inhibitors [Roche]). Cell lysates were precleared with Protein A/G Plus Agarose beads (Pierce) for 1 hr at 4°C and incubated with primary antibodies (either IGF2BP2 or DHX9) or rabbit IgG control (Santa Cruz Biotechnology) overnight at 4°C. Protein/RNA complexes were precipitated with Protein A/G Plus Agarose beads, washed three times with modified RIPA buffer, washed three times with high-salt buffer (1 M NaCl modified RIPA buffer), and then washed three times with modified RIPA buffer. Samples were then treated with Proteinase K (Invitrogen) and RNA was extracted using Trizol. The qPCR was performed as described above.

In Vivo Studies

Female athymic nude mice were purchased from Envigo. For all studies mice were housed at HMS animal facility in accordance with all NIH regulations. For intracranial tumor injection, cells were analyzed for viability using the Muse Count & Viability Reagent on the Muse Cell Analyzer (Millipore), following the manufacturer's instructions to normalize number of viable cells prior to the transplantation of 5,000 viable GSCs, transduced with either control or HIF1A-AS2 shRNA vector and stereotactically injected (2 mm right lateral, 0.5 mm frontal to the bregma, and 4 mm deep) into the brains of 6- to 8-week-old mice. Animals were sacrificed as per protocol and brain tissue was processed as described (Bronisz et al., 2014). Brain sections were imaged using a confocal microscope (Zeiss LSM710).

Data and Statistical Analysis

Functional bioinformatic analyses were performed using David Functional Annotation tool (https://david.ncifcrf.gov) and STRING v10 protein-protein interaction networks software (Szklarczyk et al., 2015). Experimental and clinical data were analyzed using the GBM-BioDP (http://gbm-biodp.nci.nih.gov) as described (Celiku et al., 2014). Clinical data were downloaded from The Cancer Genome Atlas (TCGA) data portal (https://tcga-data.nci.nih.gov/) as described in TCGA research (Network, 2013). Gene expression data included data from three platforms as follows: HT_HG-U133A (488 patient samples × 12,042 features), HuEx-1_0-st-v2 (437 patient samples × 18,631 features), and AgilentG4502A_07_1/2 (101 + 396 patient sample × 17,813 features). The data from the three platforms were aggregated (Verhaak et al., 2010).

GSC microarray data (Mao et al., 2013) were queried for cluster analysis with PAN Cancer platform data. Clinical data included partial clinical information on 564 patients. The experimental data were already pre-processed as a part of TCGA data. The genes downregulated by HIF1A-AS2 knockdown were used to predict patient outcome. Genes identified as a IGF2BP2 targets (Janiszewska et al., 2012) were queried with genes that vary coherently between P and M GSCs (Mao et al., 2013). Gene expression in the various anatomical regions of glioblastoma was analyzed using the Ivy Glioblastoma Atlas Project (http://glioblastoma.alleninstitute.org/). Data are expressed as mean ± SD. Statistical analyses were performed using the unpaired two-tailed Student's t test from GraphPad Prism software. Differences were considered statistically significant at $p < 0.05$.

SUPPLEMENTAL INFORMATION

Supplemental Information includes Supplemental Experimental Procedures, four figures, and four tables and can be found with this article online at http://dx.doi.org/10.1016/j.celrep.2016.05.018.

AUTHOR CONTRIBUTIONS

All authors assisted in drafting and revising the work, approved the final version for publication, and agree to be accountable for all aspects of the work. M.M. conceived the overall work and developed the methodology. F.R. performed in vitro and in vivo experiments. A.K.R. and S.M.L. performed in vitro experiments. K.I.A. designed the NS platform. P.I. assisted with writing the manuscript and analysis and interpretation of data. I.N. acquired patients' specimens and assisted with interpretation of data. E.A.C. acquired patients' specimens and assisted with writing the manuscript. J.G. and A.B. conceived and designed overall work, analyzed and interpreted data, and wrote the manuscript.

ACKNOWLEDGMENTS

This research was supported by NCI P01 CA69246 (to E.A.C.) and NCI 1R01 CA176203-01A1 (to J.G.).

Received: January 22, 2016
Revised: March 29, 2016
Accepted: May 2, 2016
Published: June 2, 2016

REFERENCES

Bhat, K.P., Balasubramaniyan, V., Vaillant, B., Ezhilarasan, R., Hummelink, K., Hollingsworth, F., Wani, K., Heathcock, L., James, J.D., Goodman, L.D., et al. (2013). Mesenchymal differentiation mediated by NF-κB promotes radiation resistance in glioblastoma. Cancer Cell *24*, 331–346.

Bozdag, S., Li, A., Baysan, M., and Fine, H.A. (2014). Master regulators, regulatory networks, and pathways of glioblastoma subtypes. Cancer Inform. *13* (*Suppl 3*), 33–44.

Brat, D.J., Castellano-Sanchez, A.A., Hunter, S.B., Pecot, M., Cohen, C., Hammond, E.H., Devi, S.N., Kaur, B., and Van Meir, E.G. (2004). Pseudopalisades in glioblastoma are hypoxic, express extracellular matrix proteases, and are formed by an actively migrating cell population. Cancer Res. *64*, 920–927.

Bronisz, A., Wang, Y., Nowicki, M.O., Peruzzi, P., Ansari, K.I., Ogawa, D., Balaj, L., De Rienzo, G., Mineo, M., Nakano, I., et al. (2014). Extracellular vesicles modulate the glioblastoma microenvironment via a tumor suppression signaling network directed by miR-1. Cancer Res. *74*, 738–750.

Carro, M.S., Lim, W.K., Alvarez, M.J., Bollo, R.J., Zhao, X., Snyder, E.Y., Sulman, E.P., Anne, S.L., Doetsch, F., Colman, H., et al. (2010). The transcriptional network for mesenchymal transformation of brain tumours. Nature *463*, 318–325.

Celiku, O., Johnson, S., Zhao, S., Camphausen, K., and Shankavaram, U. (2014). Visualizing molecular profiles of glioblastoma with GBM-BioDP. PLoS ONE *9*, e101239.

Chang, Y.N., Zhang, K., Hu, Z.M., Qi, H.X., Shi, Z.M., Han, X.H., Han, Y.W., and Hong, W. (2016). Hypoxia-regulated lncRNAs in cancer. Gene *575*, 1–8.

Chatel-Chaix, L., Germain, M.A., Motorina, A., Bonneil, É., Thibault, P., Baril, M., and Lamarre, D. (2013). A host YB-1 ribonucleoprotein complex is hijacked by hepatitis C virus for the control of NS3-dependent particle production. J. Virol. *87*, 11704–11720.

Chiappetta, G., Avantaggiato, V., Visconti, R., Fedele, M., Battista, S., Trapasso, F., Merciai, B.M., Fidanza, V., Giancotti, V., Santoro, M., et al. (1996). High level expression of the HMGI (Y) gene during embryonic development. Oncogene *13*, 2439–2446.

Cooper, L.A., Gutman, D.A., Chisolm, C., Appin, C., Kong, J., Rong, Y., Kurc, T., Van Meir, E.G., Saltz, J.H., Moreno, C.S., and Brat, D.J. (2012). The tumor microenvironment strongly impacts master transcriptional regulators and gene expression class of glioblastoma. Am. J. Pathol. *180*, 2108–2119.

Du, Z., Fei, T., Verhaak, R.G., Su, Z., Zhang, Y., Brown, M., Chen, Y., and Liu, X.S. (2013). Integrative genomic analyses reveal clinically relevant long noncoding RNAs in human cancer. Nat. Struct. Mol. Biol. *20*, 908–913.

Fatica, A., and Bozzoni, I. (2014). Long non-coding RNAs: new players in cell differentiation and development. Nat. Rev. Genet. *15*, 7–21.

Flynn, R.A., and Chang, H.Y. (2012). Active chromatin and noncoding RNAs: an intimate relationship. Curr. Opin. Genet. Dev. *22*, 172–178.

Frattini, V., Trifonov, V., Chan, J.M., Castano, A., Lia, M., Abate, F., Keir, S.T., Ji, A.X., Zoppoli, P., Niola, F., et al. (2013). The integrated landscape of driver genomic alterations in glioblastoma. Nat. Genet. *45*, 1141–1149.

Fusco, A., and Fedele, M. (2007). Roles of HMGA proteins in cancer. Nat. Rev. Cancer *7*, 899–910.

Godlewski, J., Krichevsky, A.M., Johnson, M.D., Chiocca, E.A., and Bronisz, A. (2015). Belonging to a network–microRNAs, extracellular vesicles, and the glioblastoma microenvironment. Neuro-oncol. *17*, 652–662.

Halliday, J., Helmy, K., Pattwell, S.S., Pitter, K.L., LaPlant, Q., Ozawa, T., and Holland, E.C. (2014). In vivo radiation response of proneural glioma characterized by protective p53 transcriptional program and proneural-mesenchymal shift. Proc. Natl. Acad. Sci. USA *111*, 5248–5253.

Huarte, M. (2015). The emerging role of lncRNAs in cancer. Nat. Med. *21*, 1253–1261.

Janiszewska, M., Suvà, M.L., Riggi, N., Houtkooper, R.H., Auwerx, J., Clément-Schatlo, V., Radovanovic, I., Rheinbay, E., Provero, P., and Stamenkovic, I. (2012). Imp2 controls oxidative phosphorylation and is crucial for preserving glioblastoma cancer stem cells. Genes Dev. *26*, 1926–1944.

Johnson, D.R., and O'Neill, B.P. (2012). Glioblastoma survival in the United States before and during the temozolomide era. J. Neurooncol. *107*, 359–364.

Jones, D.L., and Wagers, A.J. (2008). No place like home: anatomy and function of the stem cell niche. Nat. Rev. Mol. Cell Biol. *9*, 11–21.

Joseph, J.V., Conroy, S., Pavlov, K., Sontakke, P., Tomar, T., Eggens-Meijer, E., Balasubramaniyan, V., Wagemakers, M., den Dunnen, W.F., and Kruyt, F.A. (2015). Hypoxia enhances migration and invasion in glioblastoma by promoting a mesenchymal shift mediated by the HIF1α-ZEB1 axis. Cancer Lett. *359*, 107–116.

Kim, S.H., Ezhilarasan, R., Phillips, E., Gallego-Perez, D., Sparks, A., Taylor, D., Ladner, K., Furuta, T., Sabit, H., Chhipa, R., et al. (2016). Serine/Threonine Kinase MLK4 Determines Mesenchymal Identity in Glioma Stem Cells in an NF-κB-dependent Manner. Cancer Cell *29*, 201–213.

Kunej, T., Obsteter, J., Pogacar, Z., Horvat, S., and Calin, G.A. (2014). The decalog of long non-coding RNA involvement in cancer diagnosis and monitoring. Crit. Rev. Clin. Lab. Sci. *51*, 344–357.

Lathia, J.D., Mack, S.C., Mulkearns-Hubert, E.E., Valentim, C.L., and Rich, J.N. (2015). Cancer stem cells in glioblastoma. Genes Dev. *29*, 1203–1217.

Lee, T., Di Paola, D., Malina, A., Mills, J.R., Kreps, A., Grosse, F., Tang, H., Zannis-Hadjopoulos, M., Larsson, O., and Pelletier, J. (2014). Suppression of the

DHX9 helicase induces premature senescence in human diploid fibroblasts in a p53-dependent manner. J. Biol. Chem. *289*, 22798–22814.

Li, Z., Bao, S., Wu, Q., Wang, H., Eyler, C., Sathornsumetee, S., Shi, Q., Cao, Y., Lathia, J., McLendon, R.E., et al. (2009). Hypoxia-inducible factors regulate tumorigenic capacity of glioma stem cells. Cancer Cell *15*, 501–513.

Liu, B., Pang, B., Liu, H., Arakawa, Y., Zhang, R., Feng, B., Zhong, P., Murata, D., Fan, H., Xin, T., et al. (2015). High mobility group A1 expression shows negative correlation with recurrence time in patients with glioblastoma multiforme. Pathol. Res. Pract. *211*, 596–600.

Mao, P., Joshi, K., Li, J., Kim, S.H., Li, P., Santana-Santos, L., Luthra, S., Chandran, U.R., Benos, P.V., Smith, L., et al. (2013). Mesenchymal glioma stem cells are maintained by activated glycolytic metabolism involving aldehyde dehydrogenase 1A3. Proc. Natl. Acad. Sci. USA *110*, 8644–8649.

Marx, V. (2014). A blooming genomic desert. Nat. Methods *11*, 135–138.

Mathew, L.K., Skuli, N., Mucaj, V., Lee, S.S., Zinn, P.O., Sathyan, P., Imtiyaz, H.Z., Zhang, Z., Davuluri, R.V., Rao, S., et al. (2014). miR-218 opposes a critical RTK-HIF pathway in mesenchymal glioblastoma. Proc. Natl. Acad. Sci. USA *111*, 291–296.

Meacham, C.E., and Morrison, S.J. (2013). Tumour heterogeneity and cancer cell plasticity. Nature *501*, 328–337.

Minajigi, A., Froberg, J.E., Wei, C., Sunwoo, H., Kesner, B., Colognori, D., Lessing, D., Payer, B., Boukhali, M., Haas, W., and Lee, J.T. (2015). Chromosomes. A comprehensive Xist interactome reveals cohesin repulsion and an RNA-directed chromosome conformation. Science *349*, aab2276.

Mineo, M., Garfield, S.H., Taverna, S., Flugy, A., De Leo, G., Alessandro, R., and Kohn, E.C. (2012). Exosomes released by K562 chronic myeloid leukemia cells promote angiogenesis in a Src-dependent fashion. Angiogenesis *15*, 33–45.

Moore, M.J., Zhang, C., Gantman, E.C., Mele, A., Darnell, J.C., and Darnell, R.B. (2014). Mapping Argonaute and conventional RNA-binding protein interactions with RNA at single-nucleotide resolution using HITS-CLIP and CIMS analysis. Nat. Protoc. *9*, 263–293.

Nakano, I. (2014). Proneural-mesenchymal transformation of glioma stem cells: do therapies cause evolution of target in glioblastoma? Future Oncol. *10*, 1527–1530.

Network, T.C. (2013). Corrigendum: Comprehensive genomic characterization defines human glioblastoma genes and core pathways. Nature *494*, 506.

Orr, B.A., and Eberhart, C.G. (2012). Nature versus nurture in glioblastoma: microenvironment and genetics can both drive mesenchymal transcriptional signature. Am. J. Pathol. *180*, 1768–1771.

Parsons, D.W., Jones, S., Zhang, X., Lin, J.C., Leary, R.J., Angenendt, P., Mankoo, P., Carter, H., Siu, I.M., Gallia, G.L., et al. (2008). An integrated genomic analysis of human glioblastoma multiforme. Science *321*, 1807–1812.

Pastori, C., Kapranov, P., Penas, C., Peschansky, V., Volmar, C.H., Sarkaria, J.N., Bregy, A., Komotar, R., St Laurent, G., Ayad, N.G., and Wahlestedt, C. (2015). The Bromodomain protein BRD4 controls HOTAIR, a long noncoding RNA essential for glioblastoma proliferation. Proc. Natl. Acad. Sci. USA *112*, 8326–8331.

Patel, A.P., Tirosh, I., Trombetta, J.J., Shalek, A.K., Gillespie, S.M., Wakimoto, H., Cahill, D.P., Nahed, B.V., Curry, W.T., Martuza, R.L., et al. (2014). Single-cell RNA-seq highlights intratumoral heterogeneity in primary glioblastoma. Science *344*, 1396–1401.

Peruzzi, P., Bronisz, A., Nowicki, M.O., Wang, Y., Ogawa, D., Price, R., Nakano, I., Kwon, C.H., Hayes, J., Lawler, S.E., et al. (2013). MicroRNA-128 coordinately targets Polycomb Repressor Complexes in glioma stem cells. Neuro-oncol. *15*, 1212–1224.

Phillips, H.S., Kharbanda, S., Chen, R., Forrest, W.F., Soriano, R.H., Wu, T.D., Misra, A., Nigro, J.M., Colman, H., Soroceanu, L., et al. (2006). Molecular subclasses of high-grade glioma predict prognosis, delineate a pattern of disease progression, and resemble stages in neurogenesis. Cancer Cell *9*, 157–173.

Piao, Y., Liang, J., Holmes, L., Henry, V., Sulman, E., and de Groot, J.F. (2013). Acquired resistance to anti-VEGF therapy in glioblastoma is associated with a mesenchymal transition. Clin. Cancer Res. *19*, 4392–4403.

Qureshi, I.A., and Mehler, M.F. (2012). Emerging roles of non-coding RNAs in brain evolution, development, plasticity and disease. Nat. Rev. Neurosci. *13*, 528–541.

Reardon, D.A., Ligon, K.L., Chiocca, E.A., and Wen, P.Y. (2015). One size should not fit all: advancing toward personalized glioblastoma therapy. Discov. Med. *19*, 471–477.

Ricklefs, F., Mineo, M., Rooj, A.K., Nakano, I., Charest, A., Weissleder, R., Breakefield, X.O., Chiocca, E.A., Godlewski, J., and Bronisz, A. (2016). Extracellular vesicles from high grade glioma exchange diverse pro-oncogenic signals that maintain intratumoral heterogeneity. Cancer Res., canres.3432.2015.

Semenza, G.L. (2013). HIF-1 mediates metabolic responses to intratumoral hypoxia and oncogenic mutations. J. Clin. Invest. *123*, 3664–3671.

Simon, M.C., and Keith, B. (2008). The role of oxygen availability in embryonic development and stem cell function. Nat. Rev. Mol. Cell Biol. *9*, 285–296.

Singh, S.K., Hawkins, C., Clarke, I.D., Squire, J.A., Bayani, J., Hide, T., Henkelman, R.M., Cusimano, M.D., and Dirks, P.B. (2004). Identification of human brain tumour initiating cells. Nature *432*, 396–401.

Soeda, A., Hara, A., Kunisada, T., Yoshimura, S., Iwama, T., and Park, D.M. (2015). The evidence of glioblastoma heterogeneity. Sci. Rep. *5*, 7979.

Sørensen, M.D., Fosmark, S., Hellwege, S., Beier, D., Kristensen, B.W., and Beier, C.P. (2015). Chemoresistance and chemotherapy targeting stem-like cells in malignant glioma. Adv. Exp. Med. Biol. *853*, 111–138.

Suvà, M.L., Rheinbay, E., Gillespie, S.M., Patel, A.P., Wakimoto, H., Rabkin, S.D., Riggi, N., Chi, A.S., Cahill, D.P., Nahed, B.V., et al. (2014). Reconstructing and reprogramming the tumor-propagating potential of glioblastoma stem-like cells. Cell *157*, 580–594.

Szklarczyk, D., Franceschini, A., Wyder, S., Forslund, K., Heller, D., Huerta-Cepas, J., Simonovic, M., Roth, A., Santos, A., Tsafou, K.P., et al. (2015). STRING v10: protein-protein interaction networks, integrated over the tree of life. Nucleic Acids Res. *43*, D447–D452.

Takahashi, K., Yan, I.K., Haga, H., and Patel, T. (2014). Modulation of hypoxia-signaling pathways by extracellular linc-RoR. J. Cell Sci. *127*, 1585–1594.

Thrash-Bingham, C.A., and Tartof, K.D. (1999). aHIF: a natural antisense transcript overexpressed in human renal cancer and during hypoxia. J. Natl. Cancer Inst. *91*, 143–151.

Ulitsky, I., and Bartel, D.P. (2013). lincRNAs: genomics, evolution, and mechanisms. Cell *154*, 26–46.

Vassallo, I., Zinn, P., Lai, M., Rajakannu, P., Hamou, M.F., and Hegi, M.E. (2016). WIF1 re-expression in glioblastoma inhibits migration through attenuation of non-canonical WNT signaling by downregulating the lncRNA MALAT1. Oncogene *35*, 12–21.

Verhaak, R.G., Hoadley, K.A., Purdom, E., Wang, V., Qi, Y., Wilkerson, M.D., Miller, C.R., Ding, L., Golub, T., Mesirov, J.P., et al.; Cancer Genome Atlas Research Network (2010). Integrated genomic analysis identifies clinically relevant subtypes of glioblastoma characterized by abnormalities in PDGFRA, IDH1, EGFR, and NF1. Cancer Cell *17*, 98–110.

Wang, G.L., Jiang, B.H., Rue, E.A., and Semenza, G.L. (1995). Hypoxia-inducible factor 1 is a basic-helix-loop-helix-PAS heterodimer regulated by cellular O2 tension. Proc. Natl. Acad. Sci. USA *92*, 5510–5514.

Zhang, J.X., Han, L., Bao, Z.S., Wang, Y.Y., Chen, L.Y., Yan, W., Yu, S.Z., Pu, P.Y., Liu, N., You, Y.P., et al.; Chinese Glioma Cooperative Group (2013). HOTAIR, a cell cycle-associated long noncoding RNA and a strong predictor of survival, is preferentially expressed in classical and mesenchymal glioma. Neuro-oncol. *15*, 1595–1603.

Zheng, S., Houseman, E.A., Morrison, Z., Wrensch, M.R., Patoka, J.S., Ramos, C., Haas-Kogan, D.A., McBride, S., Marsit, C.J., Christensen, B.C., et al. (2011). DNA hypermethylation profiles associated with glioma subtypes and EZH2 and IGFBP2 mRNA expression. Neuro-oncol. *13*, 280–289.